

Felix Schuderer*, Michael Kircher, Birgit Stender, Thomas Bluth, Marcelo Gama de Abreu, and Olaf Dössel

Introducing a Linear Gamma Variate Fit to Measure Pulmonary Perfusion with Electrical Impedance Tomography

<https://doi.org/10.1515/cdbme-2020-3089>

Abstract: The indicator dilution method (IDM) is one approach to measure pulmonary perfusion using Electrical Impedance Tomography (EIT). To be able to calculate perfusion parameters and to increase robustness, it is necessary to approximate and then to separate the components of the measured signals. The component referring to the passage of the injected bolus through the pixels can be modeled as a gamma variate function, its parameters are often determined using nonlinear optimization algorithms. In this paper, we introduce a linear approach that enables higher robustness and faster computation, and compare the linear and nonlinear fitting approach on data of an animal study.

Keywords: Electrical Impedance Tomography, Indicator Dilution, Gamma Variate, Least Squares, Parameter Optimization, Pulmonary Perfusion

1 Introduction

Pulmonary diseases are among the most common causes of death worldwide. A reliable diagnostic method, e.g. based on imaging techniques, is the first step in a successful treatment. EIT allows functional imaging of the lungs and offers - in contrast to MRI, CT or PET - the possibility for diagnostics at bedside, combined with a high temporal resolution [1]. One method to measure pulmonary perfusion using EIT is the IDM, where a saline solution (NaCl) is injected during apnea. Due to its significantly higher conductivity compared to air or blood, the measured conductivity increases in a pixel of the reconstructed image when the injected bolus appears. The observed signal can be considered as a gamma variate function, superimposed by other signal components [3][4]. Approximating

and then extracting the pure IDM component is necessary to calculate perfusion parameters, e.g. blood flow.

In [2], a nonlinear least squares (NLS) approach is used to calculate the gamma variate's parameters for EIT. However, a linear fit has many advantages, e.g. no necessity of parameter initialization, avoiding local minima, no stability problems and faster computation. In this paper, we present a fit based on linear least squares (LLS) and compare it to the nonlinear approach based on data of a porcine study [6]. The results also allowed us to calculate temporal propagation maps of the injected saline bolus.

2 Methods

A nonlinear and a linear approach to approximate the gamma variate component of EIT signals were implemented and compared. The nonlinear fit is a modification of the method described in [2], the linear fit was developed during this work. Data of three pigs of an animal study were used for algorithm development, the method evaluation and comparison was done using all 13 pigs of the study. Two criteria were used for comparison: The root mean square error (RMSE) and the correlation between the approximated and the raw signals.

2.1 Data

The aim of the animal study was to compare pulmonary perfusion distributions in the lungs of anesthetized pigs measured with EIT and PET [6]. One part of the study included perfusion measurements using the IDM. Different ventilation states and concentrations of the injected saline solution were measured. Due to space limitations, we present only a fraction of the complete evaluation here. We focus on the ventilation states healthy lungs (both lungs optimally ventilated) and single sided ventilation, and on the concentrations of 10% and 3% NaCl in the injected saline solutions.

*Corresponding author: Felix Schuderer, Institute of Biomedical Engineering, KIT, Fritz-Haber-Weg 1, Karlsruhe, Germany, e-mail: publications@ibt.kit.edu

Michael Kircher, Olaf Dössel, Institute of Biomedical Engineering, KIT, Karlsruhe, Germany

Birgit Stender, Drägerwerk AG & Co. KGaA, Lübeck, Germany

Thomas Bluth, Marcelo Gama de Abreu, Pulmonary Engineering Group, Department of Anesthesiology and Intensive Care Medicine, University Hospital & TU Dresden, Dresden, Germany

2.2 Preprocessing

To reconstruct the EIT images, we used a linearized and normalized Gauss-Newton method. Then, we applied the same preprocessing to the EIT signals for both fitting approaches.

The pixel signals $\Delta\sigma_i(t)$ represent the local change of conductivity compared to a reference state and are influenced by the amount of air, the amount of blood and the presence of the injected bolus in the corresponding areas. With respect to our observations and [2], we assumed the signal model in equation (1). $\gamma_1(t)$ shows the first-pass of the bolus through the right heart and the lung circuit after injection, $\gamma_2(t)$ the entry of the bolus into the left heart, $d(t)$ a drift caused by indicator diffusion from the vessels into surrounding tissue and $e(t)$ measurement noise.

$$\Delta\sigma_i(t) = \gamma_1(t) + \gamma_2(t) + d(t) + e(t). \quad (1)$$

The part of a signal where the gamma variates are located is named gamma complex here. Its borders are denoted t_A and t_E , as it can be seen in Figure 1. t_A is assumed to be the indicator's arrival time in the pixel.

In a first step we eliminated noise and pulsatility effects caused by cardiac activities using a butterworth filter of order 10 with a cut-off frequency of 0.5 Hz.

Then we eliminated pixels that did not belong to areas where pulmonary vessels are expected as they are not relevant for pulmonary perfusion. For simplification, we assumed that only 50% of all pixels of an image were relevant. We calculated the amplitude of each signal and eliminated all signals with an amplitude below the median.

The last step was to eliminate the drift component $d(t)$ in the relevant signals using a piecewise approach that is explained more detailed in [7]. First of all, we determined the borders of the gamma complex. Therefore, we calculated the tangents to the maximal positive and negative slope of the signal, as they are located in the rising and falling flanks of the gamma complex. The borders then were defined as the tangents' intersection points with $\Delta\sigma = 0$. Two straight lines were fitted to the left of t_A and to the right of t_E respectively. They were connected with a third straight line between t_A and t_E . To remove the sharp edges at t_A and t_E , a butterworth low pass filter with a cut-off frequency of 0.1 Hz was applied. The resulting approximation can be subtracted from the signal to eliminate the drift. Figure 1 shows the borders of the gamma complex and the resulting approximation for $d(t)$.

2.3 Gamma variate fit

After eliminating $d(t)$ the signal shape has changed and the gamma complex has to be determined for a second time. Af-

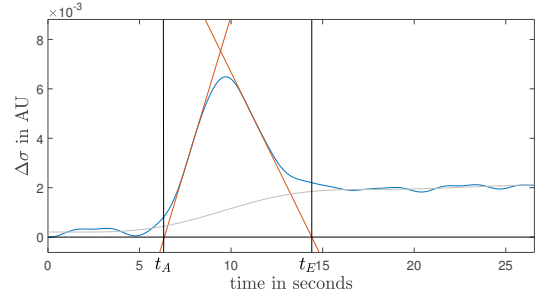


Fig. 1: Between t_A and t_E the gamma complex is located. It is determined calculating the intersection of the maximal slope tangents with $\Delta\sigma = 0$. In grey, the piecewise fitted drift component $d(t)$ is printed.

terwards we detected the signal's peak inside the gamma complex.

In pixels where only one peak was found now $\gamma_1(t)$ was fitted using the nonlinear or linear method that is described below. For both methods, only signal values around the peak were used, as they show a good SNR due to their relatively large values. This was especially necessary to achieve good results with the linear fit. More precisely we empirically determined to use signal values between $t_l + \frac{t_{max} - t_l}{2}$ and $t_{max} + 0.4s$, where t_l is the sample of the maximal positive slope and t_{max} the sample of the peak.

In pixels with two peaks, the first temporal peak and thus, $\gamma_1(t)$, was fitted. The same signal values as described above were used. Then, the approximated gamma function was subtracted from the signal. Again, the peak inside the gamma complex was detected. If the ratio of this peak's amplitude to the firstly detected peak laid above an empirically determined threshold, $\gamma_2(t)$ was fitted to the signal. In this case we assumed that the maximal slope is located in the middle between the start time t_A and the peak of $\gamma_2(t)$. All signal values between the point of maximal positive slope and the peak were used.

For each fitted gamma variate we tested fit stability by calculating the maximum value of the fitted gamma and the maximum value of the corresponding raw signal $\Delta\sigma_i$. If the fitted value was twice the raw maximum, the fitted signal was discarded.

2.3.1 Nonlinear fit

It is common to describe a gamma variate function as given in equation (2) [2].

$$\gamma(t) = A(t - t_A)^\alpha e^{-\frac{t - t_A}{\beta}}. \quad (2)$$

We used a different formulation derived in [5] by substituting time t with $t' = \frac{t-t_A}{t_{max}-t_A}$, presented in equation (3).

$$\gamma(t') = c_{max} t'^{\alpha} e^{\alpha(1-t')}, \quad (3)$$

The advantage of this formulation is that now α is the only shape describing parameter. This gave us the possibility to determine individual start values for the nonlinear fit for each signal for the parameters c_{max} , t_A and t_{max} , as they can be derived from the raw signal. For α , a fix value was used for all signals, determined empirically. The final parameter optimization was done using a nonlinear least squares method based on a trust-region-reflective algorithm.

2.3.2 Linear fit

The same gamma variate formulation as in equation (3) was used for the linear fit. Applying the logarithm yields a formulation where the parameters α and c_{max} can be optimized linearly using a linear least squares approach:

$$\ln(\gamma(t')) = \alpha(1 + \ln(t') - t') + \ln(c_{max}). \quad (4)$$

$$\begin{bmatrix} \ln(\gamma(t'_1)) \\ \ln(\gamma(t'_2)) \\ \vdots \\ \ln(\gamma(t'_n)) \end{bmatrix} = \begin{bmatrix} 1 + \ln(\gamma(t'_1)) & 1 \\ 1 + \ln(\gamma(t'_2)) & 1 \\ \vdots & \vdots \\ 1 + \ln(\gamma(t'_n)) & 1 \end{bmatrix} \cdot \begin{bmatrix} \alpha \\ \ln(c_{max}) \end{bmatrix} \quad (5)$$

Similar to the nonlinear fit it was necessary to determine the parameters t_A and t_{max} as precisely as possible from the signal, as t' must be substituted by t after the fit. t_A was determined using the tangents as described above, t_{max} by detecting the peak of the raw signal.

2.4 Comparison

We compared the total resulting approximated signals $\hat{\gamma} = \hat{\gamma}_1(t) + \hat{\gamma}_2(t) + \hat{d}(t)$ with the raw signals. We considered only the signal values inside the gamma complex to avoid corruptions of the calculated quantities due to signal parts that were not considered when fitting the components. We calculated mean values among all 13 pigs for RMSE and correlation using all signals where the fits were successful and counted the number of successful and failed fits. We also looked for the maximum and minimum values of these factors.

3 Results

Figure 2 shows an example of a fitted signal that shows two peaks and refers to the heart region. The results of the evalua-

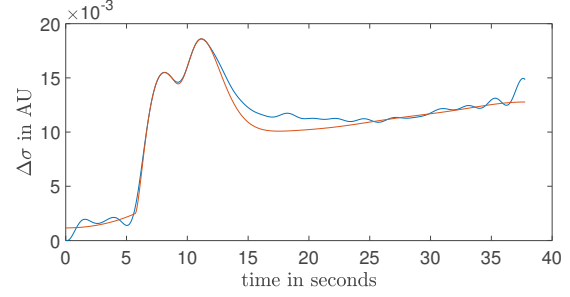


Fig. 2: The red signal approximates the measured blue signal. It consists of all three components $\gamma_1(t)$, $\gamma_2(t)$ and $d(t)$.

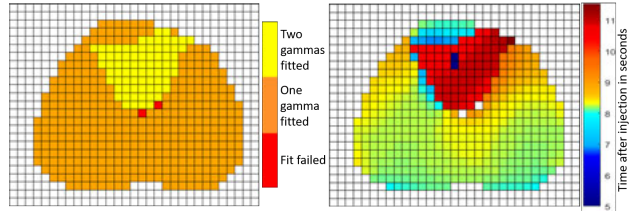


Fig. 3: Left: Pixelmap denoting how many fits were done in each pixel. Two gamma variates dominate in the heart region. Right: Temporal propagation of the injected bolus.

tion can be found in detail in table (1).

The approximated signals show a low mean RMSE between $0.81e^{-3}$ and $2.95e^{-3}$ for the linear and nonlinear fit. The correlation is for all measurements approximately 0.97. As expected the linear fit is more robust and shows a lower mean number of failed fits as well as lower maximum and minimum values of failed fits. On the other hand RMSE and correlation show slightly worse results in general and a larger variance for the linear fit. Nevertheless, the differences in RMSE and correlation are very small when comparing the linear and the nonlinear fit.

When reducing the concentration of NaCl from 10% to 3%, the RMSE becomes better, the correlation stays unchanged for both, the linear and the nonlinear fit. However, the number of failed fits increases especially for the nonlinear fit. Thus, the linear fit seems to be less sensitive to changes of the NaCl concentration. We observed this behavior also with the other concentrations of the study we cannot present here.

4 Discussion

To summarize it can be said that the linear fit shows a higher robustness compared to the nonlinear fit. However, this robustness goes hand in hand with slightly worse fitting results considering RMSE. When looking at correlation, the differences are negligible small. One reason why also the nonlinear fit

Tab. 1: Mean, maximum and minimum values among 13 pigs for different ventilation states and concentrations of NaCl for the number of successful and failed fits, RMSE and correlation between raw and approximated signals. In each column the left side shows the results of the nonlinear fit, the right side the results of the linear fit.

	Healthy lungs NaCl 10%		Healthy lungs NaCl 3%		Single sided ventilation NaCl 10%		Single sided ventilation NaCl 3%	
No. successful fits mean	694.54	694.54	710.85	710.85	748.69	748.69	793.54	793.54
No. successful fits max/min	726/666	726/666	771/660	771/660	828/691	828/691	872/740	872/740
No. Failed fits mean	3.85	0.77	11.15	2.08	6.00	2.15	9.38	1.54
No. Failed fits max/min	13/0	2/0	44/0	15/0	30/1	23/0	26/1	7/0
RMSE mean 10^{-3}	1.94	2.73	0.81	0.94	2.15	2.95	0.84	1.00
RMSE max/min 10^{-3}	2.69/1.48	4.06/1.66	0.48/1.30	1.16/0.58	3.31/1.39	1.60/3.96	1.77/0.55	1.99/0.69
RMSE variance 10^{-6}	2.82	3.77	0.45	0.50	3.72	5.76	0.61	0.72
Correlation mean	0.97	0.97	0.97	0.96	0.97	0.97	0.97	0.97
Correlation max/min	0.98/0.95	0.98/0.94	0.98/0.92	0.98/0.95	0.98/0.95	0.98/0.95	0.99/0.93	0.98/0.91
Correlation variance 10^{-3}	1.26	0.98	1.27	1.03	1.11	0.89	1.05	0.90

yields good result is supposed to be that an individual parameter initialization was done for each signal with the methods described above. This avoids failed fits.

The robustness of the fits varies among animals. This can be explained by different signal quality in the measurements and varying anatomy of the pigs. The described two peak behavior could not be observed in all pigs. When two peak pixels existed, they mainly appeared in the region where the heart is located anatomically, but also in a lower part of the image where we assumed the aorta. This can be seen exemplarily for one pig in figure 3 left, where a pixelmap shows the number of fitted gamma variates in each pixel. This is why we state that $\gamma_2(t)$ refers to the bolus in the right heart and when it is ejected into the body. The number of fitted gamma variates in each pixel can be used to classify which pixels belong to the heart region, what is necessary e.g. to eliminate these pixels when comparing EIT to PET.

As mentioned above, separating the signal components finally allowed us to calculate perfusion parameters. Blood flow was determined using the slope method described in [2], blood volume determined by calculating the area under the fitted curve without drift. Furthermore we were able to determine propagation times of the injected bolus and thus, of the blood, too. For many pigs it was possible to observe the bolus from its injection through the lungs up to the point where it passes the aorta. Figure 3 right shows a resulting temporal propagation map.

Author Statement

Research funding: The Institute of Biomedical Engineering received funds from Drägerwerk AG & Co. KGaA for the cooperation project of Michael Kircher. The animal study was funded by Drägerwerk AG & Co. KGaA.

References

- [1] Teschner E, Imhoff M, Leonhardt S. Electrical Impedance Tomography: The realisation of regional ventilation monitoring (Booklet). 2nd ed. Lübeck: Drägerwerk AG & Co. KGaA; 2015.
- [2] Borges J, Suarez-Sipmann F, Bohm S, et al. Regional lung perfusion estimated by electrical impedance tomography in a piglet model of lung collapse. *Journal of Applied Physiology* 2012;112:225–236
- [3] Meier P, Zierler K. On the Theory of the Indicator-Dilution Method for Measurement of Blood Flow and Volume. *Journal of Applied Physiology* 1954;6:731–744
- [4] Thompson H, Starmer C, Whalen R, et al. Indicator Transit Time Considered as a Gamma Variate. *Circulation research* 1964;14:502–515
- [5] Madsen M. A simplified formulation of the gamma variate function. *Physics in Medicine & Biology* 1992;37:1597–1600
- [6] Vivona L, Braune A, Bluth T, Kiss T, Kircher M, Bozsak C, et al. Variable Ventilation Is Superior to Conventional Recruitment for Reversal of Atelectasis in Anesthetized Pigs. *American Journal of Respiratory and Critical Care Medicine* 2018;197:A5122
- [7] Kircher M, Schuderer F, Stender B, Dössel O. Nonlinear and Piecewise Fitting of Indicator Enhanced EIT signals: Comparison of Methods. *Innovative digitale Verarbeitung bioelektrischer und -magnetischer Signale - Workshop Biosignalverarbeitung 2020*
- [8] Kim J, Leira E, Callison R, Ludwig B, Moritani T, Magnotta V, Madsen M. Toward fully automated processing of dynamic susceptibility contrast perfusion MRI for acute ischemic cerebral stroke. *Computer Methods and Programs in Biomedicine* 2010;98:204–213